Varendra International Journal for Interdisciplinary Research 2025: 1(2), 7-18

ISSN: 3078-1017 (Online). 3078-7009 (Print)

https://doi.org/10.64296/vijir.v1i2.04
Received: June 10, 2025; Revised: September 15, 2025; Accepted: October 21, 2025

Skin Disease Detection and Classification of Actinic Keratosis and Psoriasis Utilizing Deep Transfer Learning

Fahud Ahmmed[1], Md. Zaheer Raihan[1], Kamnur Nahar[1], D.M. Asadujjaman[1,2*], Md. Mahfujur Rahman[1], Abdullah Tamim[1],
[1]Department of Computer Science and Engineering, Varendra University, Rajshahi, Bangladesh
[2]Department of Computer Science & Engineering, Khulna University of Engineering & Technology
[*]Corresponding Author: asadujjaman@vu.edu.bd

ABSTRACT

Skin diseases can arise from infections, allergies, genetic factors, autoimmune disorders, hormonal imbalances, or environmental triggers such as sun damage and pollution. Skin diseases such as Actinic Keratosis and Psoriasis can be fatal. These are treatable if identified early. However, its diagnostic methods are expensive and not widely accessible. In this study, a novel and efficient method for diagnosing skin diseases using deep learning techniques has been proposed. This approach employs multiple modified Convolutional Neural Network (CNN) models like DenseNet169, DenseNet201 and VGG16. Soft voting ensemble strategy is applied to combine the strengths of individual models to get better result. These models include several convolutional layers. The models have been employed using ImageNet weights and modified top layers. The top layers are modified by fully connected layers and a final softmax activation layer to obtain the result. The dataset analyzed is publicly available and titled "Skin Disease Dataset". The CNN architecture does not include augmentation by default; data augmentation is typically performed during preprocessing prior to model training. The proposed methodology achieved 93.11% accuracy using the ensemble strategy, demonstrating reliability in classifying skin diseases. The modified pre-trained models showed promising results, increasing its potential for real-world applications.

Keywords: Skin Cancer, Actinic Keratosis, Psoriasis, CNN, DenseNet201, Ensemble

1. Introduction

Artificial Neural Networks (ANN), Machine Learning[13, 20], and Deep learning[14–19] have transformed dermatology by offering innovative methods for diagnosing, classifying, and treating skin diseases. Inspired by human brain architecture, ANNs efficiently manage complex data sets and interpret visual information, making them valuable for dermatological diagnoses. The skin covers the body and serves essential functions, including protection from physical, chemical, and biological threats. Skin diseases are common health issues faced by underprivileged populations in many countries [1]. WHO estimates that approximately 1.8 billion individuals are affected by skin diseases at any given time [2]. Skin diseases may result in skin cancer. Annually, 2 to 3 million non-melanoma skin cancers and 132,000

melanoma skin cancers are diagnosed worldwide [3]. The impact of disorders is influenced by climate, economic conditions, literacy levels, and the cultural and social lifestyles of communities across different geographic areas. Bangladesh experiences a high occurrence due to its humid climate and growing population. Many patients pursue treatment late due to a lack of awareness about the disease. According to Chittagong Medical College Hospital of Chittagong district in Bangladesh, more than 40,000 people were affected by skin diseases between the periods of 2003 and 2011 [4]. In the outdoor of Adamdighi Upazila Health & Family Welfare Complex of Bogra district, 15.38% of the total 1,54,843 patients were suffering from various forms of skin diseases in 2001 [5]. Dermatology now incorporates artificial neural networks to analyze various data, including patient history, symptoms, laboratory test results, and crucially, images or scans of skin lesions. ANN can recognize complex patterns and features effectively. The ANN classifies, diagnoses, and predicts skin diseases with high accuracy.

2. Related study

A recent study by Van-Dung Hoang et al. found that the EfficientNetB4-CLF model achieved an accuracy of 89.97%, a recall of 86.13%, and a false positive rate of 0.39%. DenseNet 169 outperforms EfficientNetB4 in image classification. ImageNet supplied the pre-trained network to CNNs. CyclicLR was employed to adjust the learning rate periodically. Backpropagation updated the weight values in the CNN architecture. It used 24,530 images resized to 256x192px, allocated as 10% test data, 80% train data, and 10% validation data [6]. Sadia Ghani Malik, Syed Shahryar Jamil, Abdul Aziz, and others developed a robust skin disease detection and classification system using deep neural networks, as detailed in their paper titled "High-Precision Skin Disease Diagnosis through Deep Learning on Dermoscopic Images." This paper proposes a deep neural network based on a seven-layer CNN architecture. It achieved 87.64% accuracy in tests utilizing the ISIC dataset of dermoscopic images [7]. Zhang et al. aimed to enhance skin disease diagnosis by integrating deep neural networks with human knowledge. The system achieved an accuracy of 87.25%, with a standard deviation of 2-5%, utilizing dermoscopy images. GoogleNet InceptionV3, pre-trained on over 1 millionimages, was utilized to improve their model [8]. In December 2019, the report titled “Dermatological Classification Using Deep Learning of Skin Images and Patient Background Knowledge” was authored by K. Sriwong, S. Bunrit, K. Kerdprasop, and Nittaya Kerdprasop. This study examines deep learning models utilizing pre-trained networks, recurrent neural networks, and CNNs, applied to image data and patient-specific background knowledge. They improved classification accuracy from 79.29% to 80.39% [9]. Our proposed methodology offers enhanced efficiency compared to previously suggested methodologies for deep learning models.

3. Methodology

This study evaluates dermatological images of skin disease using deep learning models for high-precision classification. DenseNet169, DenseNet201, and VGG16 were trained and tested separately for cancer detection and classification. Models’ performance was evaluated using confusion matrices, ROC curves, F1-scores, and overall accuracy.

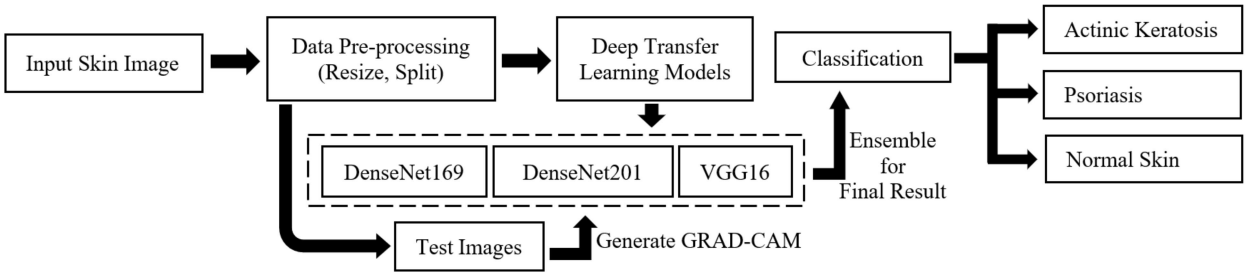

Figure 1: Workflow diagram of classification process of multiple classes

3.1. Data Description

We utilized the "Skin Disease Dataset," comprising a total of 2,400 photos across all categories. This dataset is evenly distributed and balanced. The dataset comprises photos from three classes, each containing a total of 800 samples. The dataset has been partitioned into two segments: test data and training data. The test dataset has 150 photos per class, representing 18.8% of the total data for that class, while the training dataset contains 650 images per class, accounting for 81.2% of the total data for that class. Our dataset can be obtained from public resources labeled "Skin Disease Dataset," which has thousands of data entries [10]. Table I illustrates the distribution, while Figure. 1. depicts the ratio of each disease class in our bespoke dataset. The data training process in machine learning is the phase in which a model acquires patterns from the training data. Throughout this procedure, the model is populated with input data attributes and their corresponding output labels. It subsequently readjusts its parameters and weights to minimize the discrepancy between its predictions and the actual labels. In our reviewed literature, we saw them working with multiple classes, we have picked 3 classes manually to classify them. Moreover, the model's learning process necessitates meticulous

Table 1: Details of Dataset

Class	**Image/Class**	**Dataset splitting**	
		Train	**Test / Validation**
Actinic Keratosis	800	650	150
Psoriasis	800	650	150
Normal	800	650	150

attention to data quality and parameter optimization to attain optimal outcomes. Our methodology exclusively focuses on the detection and classification of dermatological conditions.

3.2. Data Pre-processing

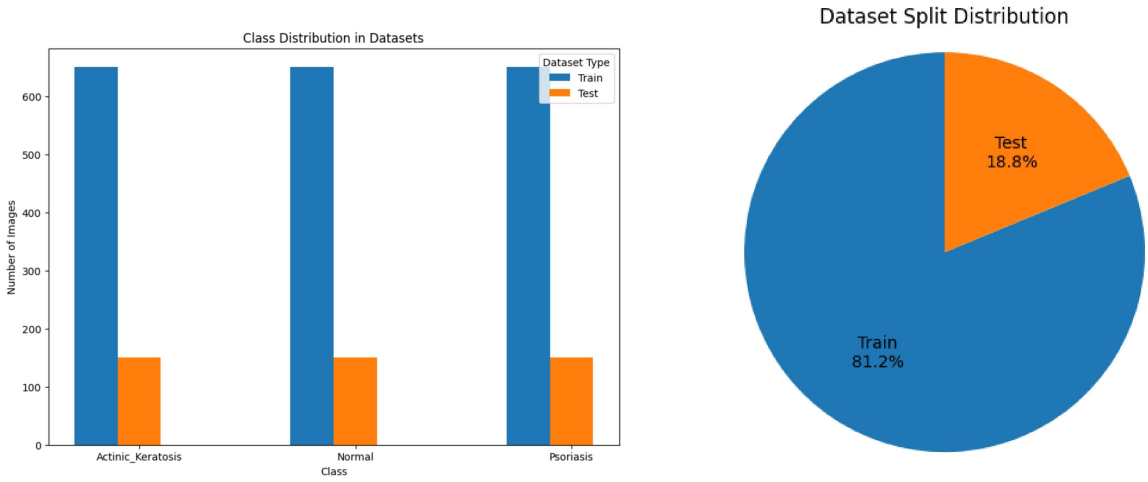

Figure 2: Dataset Distribution

Our dataset is divided into two categories with an approximate 81:19 ratio. The models are trained on the training images, while the test images are used to assess their performance. Before passing into the system, all images are preprocessed. Since Artificial Neural Networks (ANNs) require input of a fixed size, the images are resized to 224 × 224 pixels to maintain consistency. We manually split and balanced the dataset to ensure clinical validity. To enhance model generalization and reduce overfitting, we applied several data augmentation techniques. These include rescaling

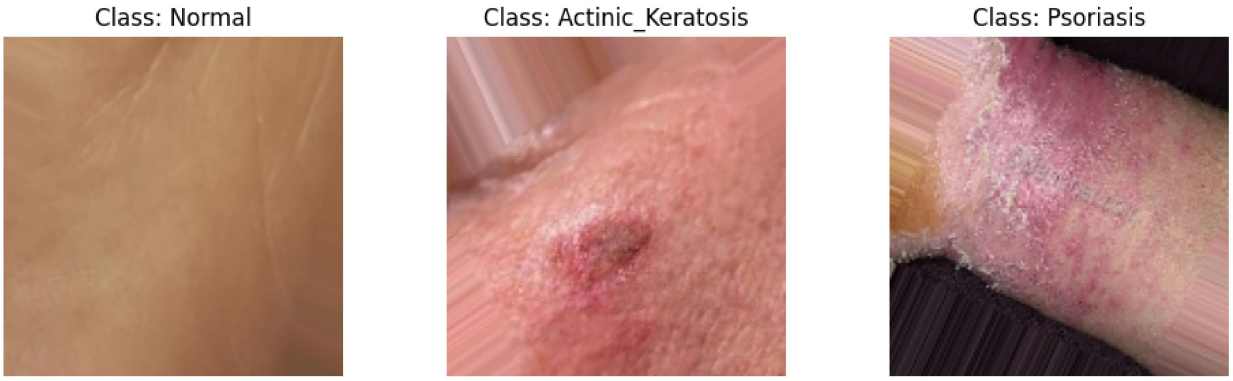

Figure 3: Sample images of the Dataset

pixel values to a 0-1 range by dividing by 255, as well as random transformations such as rotations up to 40 degrees, horizontal flipping, shearing up to 0.2 radians, height and width shifts up to 20%, and zooming up to 20%. These augmentations were implemented using ImageDataGenerator of Keras, simulating real-world image variability. Figure 2 showcases representative samples from our dataset.

However, the data preprocessing step prepares the images for training by combining resizing, augmentation, and normalization techniques, thereby enhancing the model's ability to generalize and handle diverse scenarios.

3.3. Training Deep Transfer Learning Models

The essential elements of every CNN model comprise convolutional layers, pooling layers, activation functions, fully connected layers, and an output loss layer. CNNs are distinguished for their outstanding efficacy in visual and natural language tasks.

3.3.1. DenseNet169

This convolutional neural network is characterized by dense connections, where each layer receives input from all preceding layers. This structure promotes feature reuse and ensures smooth gradient flow. In our proposed method, a pre-trained DenseNet169 model is employed for feature extraction, with its convolutional base frozen during training to preserve learned features. A custom classification head is appended, consisting of a Flatten layer followed by a Dense layer with 256 units and ReLU activation. To mitigate overfitting, a Dropout layer with a rate of 0.5 is included. The final output layer comprises 5 nodes with softmax activation to support multi-class classification. The model is compiled using the Adam optimizer with a learning rate of 0.0001 and categorical cross-entropy as the loss function.

3.3.2. DenseNet201

Building upon the DenseNet169 architecture, DenseNet201 introduces additional layers to capture more complex and abstract feature representations, while maintaining the efficiency of gradient flow and parameter reuse. In this approach, the pre-trained DenseNet201 model is similarly used as a frozen feature extractor. The classification head mirrors that of the DenseNet169 configuration: a Flatten layer, a Dense layer with 256 ReLU-activated units, a Dropout layer with a 0.5 rate, and an output Dense layer with 5 softmax-activated nodes for classification. The model is also compiled using the Adam optimizer (learning rate of 0.0001) and categorical cross-entropy as the loss function.

3.3.3. VGG16

The model is created by the Visual Geometry Group at the University of Oxford, and is a prominent convolutional neural network architecture. Feature extraction in VGG16 involves employing the network to recognize and specify the

most salient characteristics from input images. The VGG16 architecture exhibits a simple and efficient design, with 16 weight layers, 13 convolutional layers, and 3 fully connected layers. The classification head has been modified for the proposed VGG16 architecture. The revised head has a Flatten layer, two interconnected dense layers of 1024 and 512 units with ReLU activation respectively, succeeded by a final softmax layer with 3 nodes for classification output. The VGG16 was primarily developed to examine the influence of depth on deep neural networks employed for image classification applications. This is a descriptive overview of the Models' Architecture: Input Layer: All three models are designed to accept RGB input images of fixed dimensions (224×224 pixels), ensuring consistency during both training and inference phases.

3.4. Fully Connected Layers

To enable multi-class classification, each model is equipped with a custom classification head. This head includes two Dense layers of 512 and 1024 units with ReLU activation, followed by a final Dense layer with 3 output nodes using softmax activation, corresponding to the three target classes.

3.4.1. Activation Functions

The ReLU (Rectified Linear Unit) activation function is applied in the convolutional and fully connected layers (excluding the output layer). ReLU introduces non-linearity into the model and is computationally efficient, which enhances learning performance.

$$\text{ReLU}(x) = \max(0, x) \tag{1}$$

The softmax activation function is utilized in the output layer to convert the raw output logits into probability distributions across the three classes, facilitating effective multi-class classification.

$$\text{softmax}(x_i) = \frac{e^{x_i}}{\sum_j e^{x_j}} \tag{2}$$

3.4.2. Loss Functions

The models are trained using the categorical cross-entropy loss function, which quantifies the difference between the predicted probability distribution and the actual class labels. This loss function is well-suited for multi-class classification tasks, especially when handling uncertain predictions, and helps optimize overall model performance.

$$L(y, \hat{y}) = -\sum_{i=1}^{c} y_i \log(\hat{y}_i) \tag{3}$$

All models have been fine-tuned specifically for the classification of skin disease dermatological images. Their architectures are designed to effectively capture rich and discriminative image features, although this comes with an associated increase in computational complexity. Figure 4 illustrates the modified architecture of the employed pre-trained models, with the feature extraction component and the custom classification head distinctly highlighted.

3.5. Hyperparameters

Hyperparameters in CNNs encompass input size, activation functions, learning rate, batch size, epochs, optimizer, and dropout rate, all of which significantly influence model learning and performance. The learning rate regulates parameter updates, whereas dropout mitigates overfitting. Table 2 presents the hyperparameters utilized in the experimental model. To interpret the model's predictions, a custom Grad-CAM (Gradient-weighted Class Activation Mapping) function was implemented. This technique visualizes the regions of an image that the model emphasizes during classification. It operates by computing the gradients of the final convolutional layer to produce a class-specific heatmap, which is then overlaid on the original image using a custom display_GRAD_CAM function. Additionally, a GradCAMCallback was employed to automatically generate and save these visualizations at the end of each training epoch.

Table 2: Parameters of models for different stages.

Parameters	Binary Class Models
Input Size	224 × 224
Batch size	32
No. of Epochs	100
Optimizer	Adam
Learning Rate	0.0001
Activation	softmax

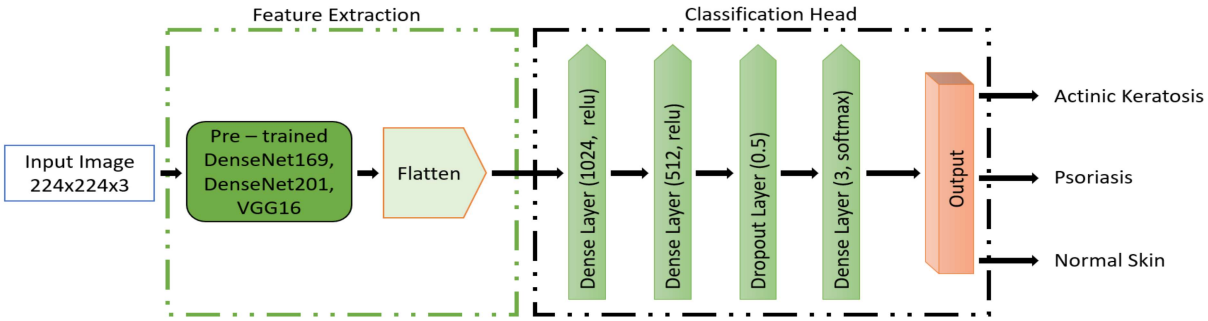

Figure 4: Modified Model Architecture

3.6. Performance Evaluation Metrices

To evaluate classification performance, several metrics are employed, including classification accuracy, specificity, precision, recall, and F1-score. These metrics provide a comprehensive assessment of the model's effectiveness. Definitions for each of these measures are presented in Equations (4) to (8).

$$\text{Accuracy} = \frac{TP + TN}{TP + FP + TN + FN} \times 100\% \tag{4}$$

$$\text{Specificity} = \frac{TN}{TN + FP} \times 100\% \tag{5}$$

Precision is a metric that evaluates the classifier's ability to correctly identify positive instances among all instances predicted as positive. It reflects how many of the predicted positive cases are actually true positives.

$$\text{Precision} = \frac{TP}{TP + FP} \times 100\% \tag{6}$$

Recall measures the proportion of actual positive instances that are correctly identified by the classifier. It reflects the model's ability to detect all relevant positive cases in the dataset.

$$\text{Recall} = \frac{TP}{TP + FN} \times 100\% \tag{7}$$

F1-score combines precision and recall into a single metric by calculating their harmonic mean. It provides a balanced evaluation of the classifier's performance, especially in cases of class imbalance. An F1-score closer to 1 indicates strong performance with high precision and recall, while a score closer to 0 reflects poor predictive capability.

$$\text{F1-score} = \frac{2 \times \text{Precision} \times \text{Recall}}{\text{Precision} + \text{Recall}} \times 100\% \tag{8}$$

where, TP, TN, FP, and FN represent the true-positive, true-negative, false-positive, and false-negative, respectively.

4. Results and Discussion

The disease detection rate, commonly referred to as the diagnostic rate, is a crucial metric in the fields of epidemiology and public health. The proposed model has demonstrated a substantial outcome in our analysis. The Receiver Operating Characteristic (ROC) curve, Confusion Matrix, and classification reports, encompassing F1-Score, Precision, and Recall, are calculated herein to thoroughly evaluate the performance of the proposed. Figure 5 and Figure 6 exhibit the confusion matrix and the ROC curve, respectively. Meanwhile, the complete classification reports summarizing f1-score, recall, and precision for each class are documented in Table 3. The Confusion Matrix revealed a significantly

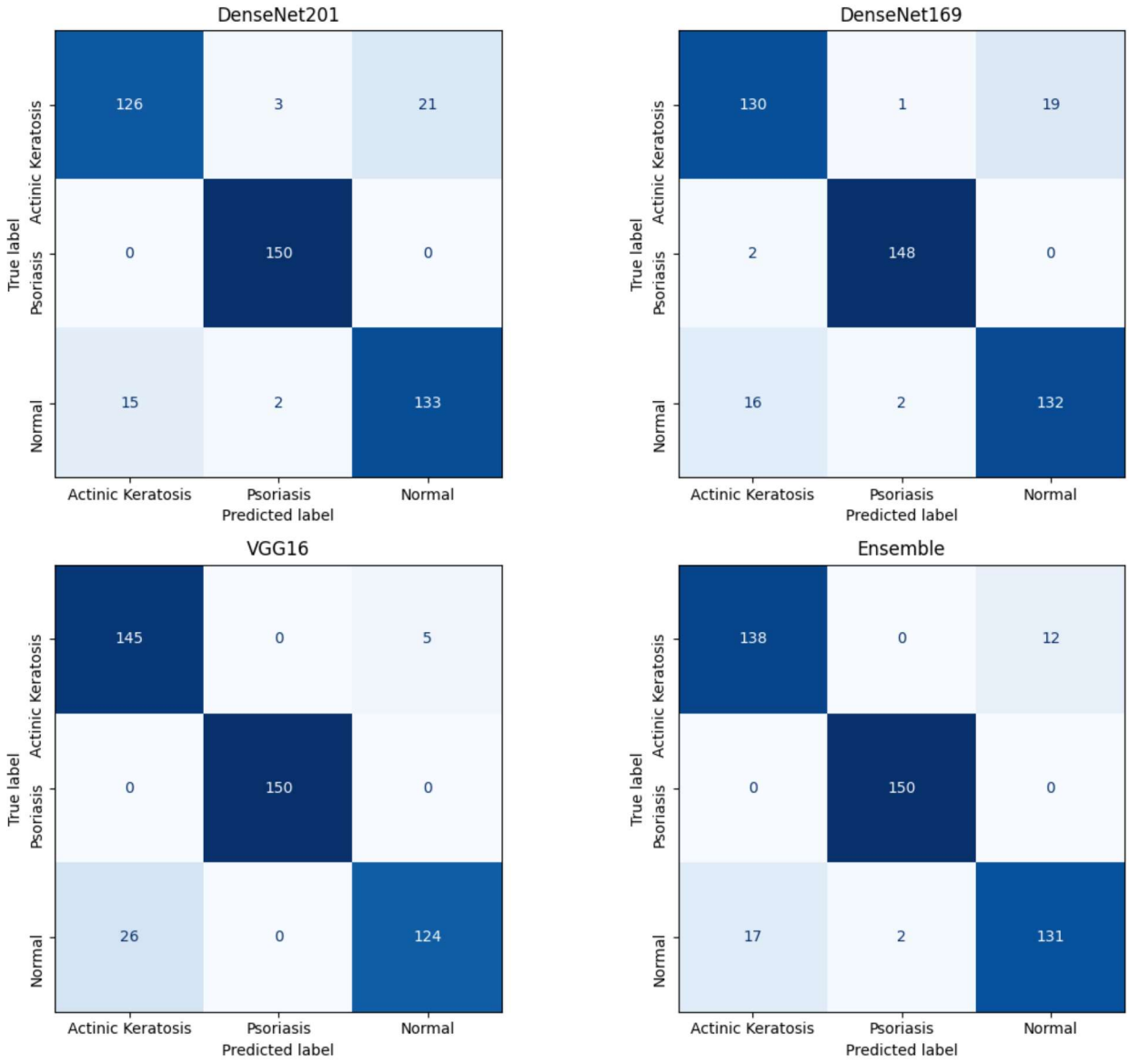

Figure 5: Confusion Matrix analysis for multiple models and ensemble strategy

high number of correct classifications along the main diagonal, showing the models' accuracy in correctly predicting the respective disease categories with minimal misclassification errors. The ROC curve analysis further validated the models' classification capability. All three models and ensemble approach got minimum Area Under Curve (AUC) value of 0.9521 and a maximum AUC value of 1.000, indicating exceptional differentiating capability between classes

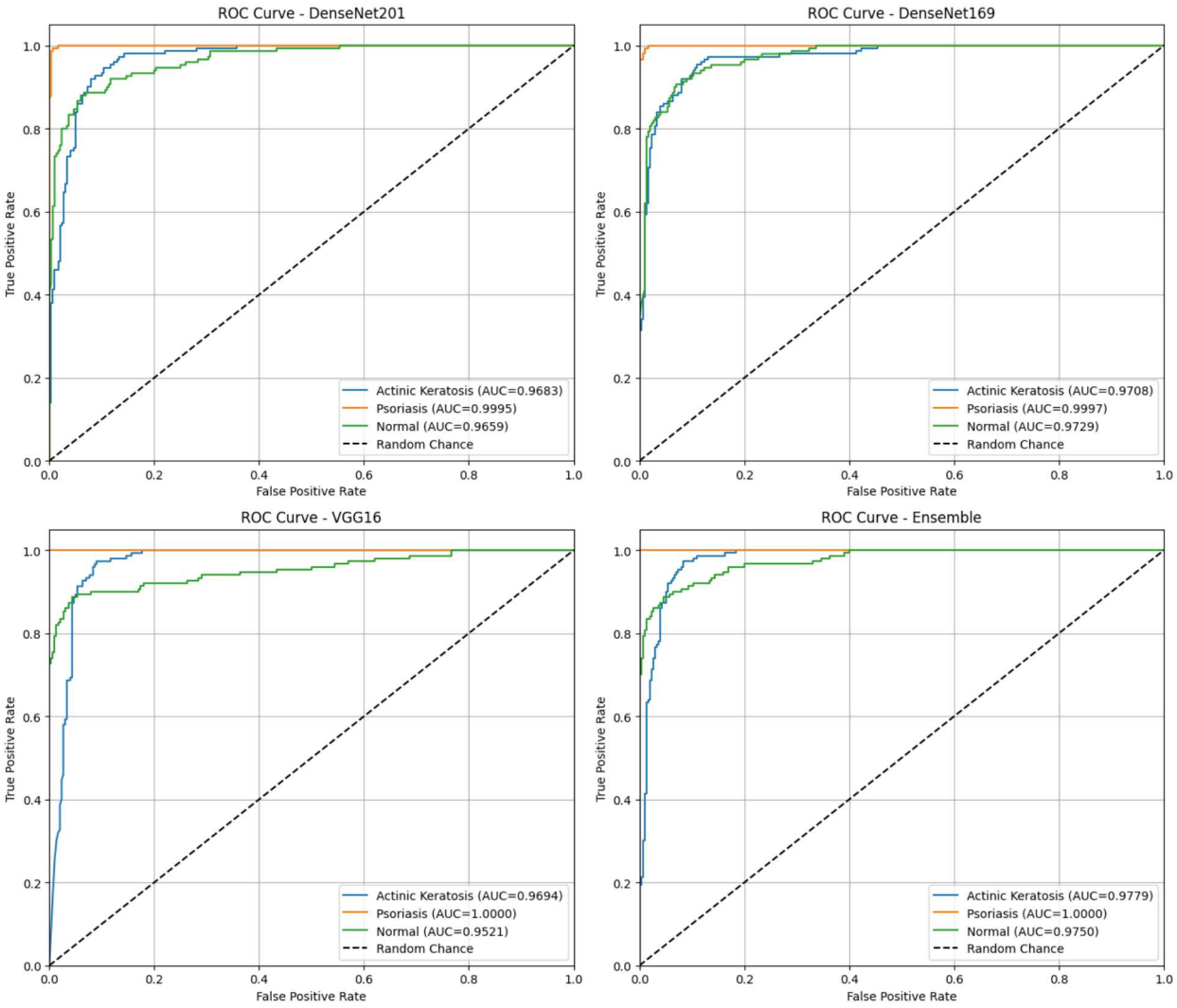

Figure 6: ROC Curve analysis for multiple models and ensemble strategy

across colon and lung cancer types. Beyond numerical performance metrics, Grad-CAM visualizations were employed

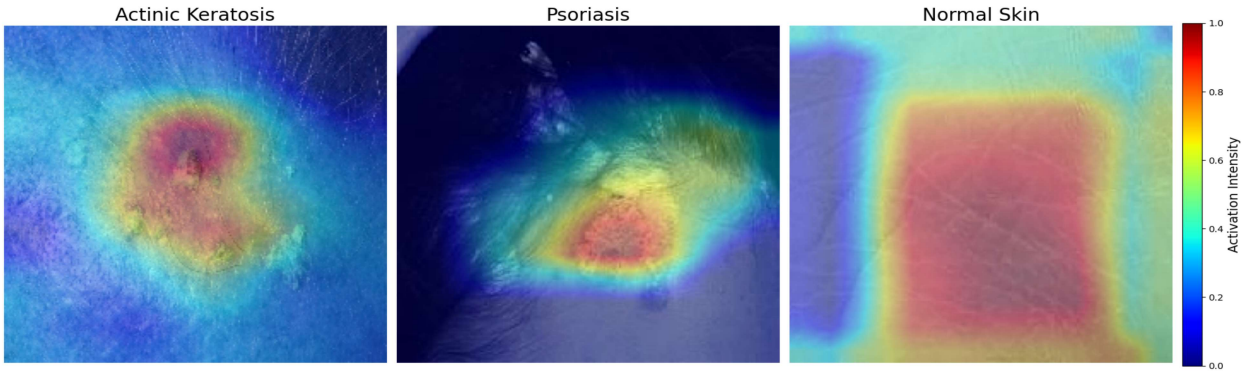

Figure 7: Grad-CAM Visualization Over Multiple Classes

to interpret the models' decision-making processes. As illustrated in Figure 7, the Grad-CAM heatmaps highlight the specific regions within the dermatological images that the models focus on during prediction. These heatmaps effectively capture distinctive tissue patterns, with areas of high importance shown in warmer colors (red, yellow) and less relevant regions displayed in cooler tones (blue, green). Such visual explanations improve the transparency of the deep learning models and reinforce their potential for clinical application. A comparative performance analysis with

Table 3: Classification Report of Multiple Model for each class

Class	DenseNet169			DenseNet201		
	Precision	Recall	F1-Score	Precision	Recall	F1-Score
Actinic Keratosis	0.88	0.87	0.87	0.89	0.84	0.87
Psoriasis	0.98	0.99	0.98	0.97	1.00	0.98
Normal	0.87	0.88	0.88	0.86	0.89	0.88
Accuracy	91.11%			90.89%		
Class	VGG16			Ensemble		
	Precision	Recall	F1-Score	Precision	Recall	F1-Score
Actinic Keratosis	0.85	0.97	0.90	0.89	0.92	0.90
Psoriasis	1.00	1.00	1.00	0.92	0.87	0.89
Normal	0.96	0.83	0.89	0.99	1.00	0.99
Accuracy	92.89%			93.11%		

prior studies highlights the effectiveness of the proposed method. Van-Dung Hoang et al. reported 89.97% accuracy using EfficientNetB4-CLF, while Sadia Ghani Malik et al. achieved 87.64% with a seven-layer CNN on the ISIC dataset. Zhang et al. reached 87.25% using InceptionV3 with expert knowledge integration, and K. Sriwong et al. improved accuracy from 79.29% to 80.39% by combining CNNs with patient data. In contrast, our proposed approach achieved a higher accuracy by ensembling the strengths of pre-trained DenseNet169, DenseNet201 and VGG16 models, demonstrating its superior performance.

However, in this study, all individual models surpassed previous works' accuracies, and the ensemble model exceeded 93.11%, setting a new benchmark in skin disease classification. Table 4 presents a comparative study of our suggested method and already established methodologies, indicating that our approach yields significant results, surpassing those of certain recent studies in the relevant field. The experimental results demonstrate top-notch classification performance

Table 4: Performance comparison of different skin disease classification models

Reference	Data	Total Classes	Model	F1-Score	Precision	Recall	Accuracy
[6]	850	7	EfficientNetB4	-	0.89	0.86	89.97%
			InceptionV3	-	0.86	0.81	86.95%
			ResNet-50	-	0.86	0.81	87.61%
			DenseNet169	-	0.87	0.84	88.46%
[9]	132	Basal cell carcinoma	ResNet-50	0.88	0.88	0.87	87.25 ± 2.24%
		Melanocytic nevus		0.89	0.89	0.88	
		Psoriasis		0.88	0.88	0.88	
		Seborrheic keratosis		0.80	0.79	0.80	
[11]	282	Acne	Custom CNN	-	0.86	0.67	83.00%
		Eczema		-	0.43	0.60	
		Psoriasis		-	0.60	0.60	
		Rosacea		-	0.50	0.24	
[12]	1,116	Actinic Keratosis	MobileNetV2	0.83	0.83	0.83	90.62%
		Psoriasis		0.90	0.88	0.93	
		Acne Vulgaris		0.80	0.73	0.89	
		Nail Fungus		0.95	1.00	0.90	
		Seborrheic Keratoses		0.96	1.00	0.92	
Proposed Approach	2,400	Actinic Keratosis	DenseNet169	0.92	0.92	0.91	91.11%
		Psoriasis	DenseNet201	0.91	0.91	0.91	90.89%
		Normal	VGG16	0.92	0.94	0.93	92.89%
			Ensemble	0.93	0.93	0.93	93.11%

across all three fine-tuned CNN models, including DenseNet169, DenseNet201, and VGG16. Among them, VGG16 achieved the highest single classification accuracy of 92.89%, closely followed by DenseNet169 and DenseNet201 with 91.11% and 90.89%, respectively. These results point to the power of transfer learning when working with meticulously curated medical image datasets in that even relatively shallower networks like VGG16 can compete with very deep architectures.

To attain even higher performance and robustness, an ensemble learning method was used by soft voting, wherein the output of all three CNN models was combined. The ensemble method achieved an accuracy of 93.11%, which was higher than the performance of all the individual models. The soft voting technique works by averaging the predicted class probabilities for all models and then predicting the final output based on the highest combined probability. This approach utilizes the complementary strengths of different architectures, reduces model-dependent biases, and improves the generalization capability of the system. The success of the ensemble highlights the advantage of collective decision-making in deep learning, especially in medical imaging, where small variations in tissue patterns can affect diagnostic effectiveness. By aggregating the views of multiple CNNs, the ensemble reduces variance and protects against overfitting to idiosyncratic features picked up by a single model. Furthermore, the integration of interpretability tools like Grad-CAM offers a critical layer of transparency in decision-making. Grad-CAM heatmaps visually accentuate the regions in dermatological images that contribute to the model's predictions, offering insights into learned features. This interpretability not only strengthens clinical trust but also facilitates model verification and refinement by clinicians.

Overall, the findings of this study confirm that transfer learning, in conjunction with ensemble techniques and visual explanation tools, is a viable framework for classifying medical images. The proposed approach not only realizes high accuracy but also addresses the increasing demand for interpretable and clinically reliable AI solutions in medicine.

5. Conclusion

Identifying skin disorders will aid in lowering death rates, rates, preventing disease spread, and mitigating the severity of the condition. Conventional clinical techniques for diagnosing skin disorders entail numerous costly and time-intensive processes. Image processing techniques facilitate the advancement of automated dermatological screening at an early stage. Consequently, feature extraction is crucial for the effective classification of dermatological conditions. The primary objective of this study was to create an accurate and interpretable deep learning model for classifying skin disease from dermatological images. This work is intended to compare the performance of a few of the current state-of-the-art convolutional neural networks, namely DenseNet169, DenseNet201, and VGG16, in identifying and classifying three skin diseases. By leveraging transfer learning on a chosen set of dermatological images, the models learned useful visual features from raw input data without needing to employ human-guided feature extraction. The comparative analysis presented the highest individual accuracy of every architecture with VGG16 coming in at 92.89%, followed very closely by DenseNet169 and DenseNet201. To the surprise of everyone, the ensemble learning approach, where predictions from all three models were made and then aggregated using soft voting, resulted in the highest overall classification accuracy of 93.11%, representing the strength and enhanced generalization effect via model fusion methods. Transfer learning played a vital role in enhancing model convergence and performance, especially based on the small size and limited variability of annotated medical image datasets. Furthermore, Grad-CAM visualizations provided interpretability to models by highlighting important regions of dermatological images that guided classification predictions. The component is vital for gaining clinical acceptance and ensuring model transparency in real diagnostic use cases. Overall, the study confirms that pre-trained CNNs, ensemble learning, and interpretability tools constitute an effective pipeline for automatic skin disease classification. The proposed framework achieves good generalization and predictive stability, thereby qualifying as an excellent resource in enabling proper and early diagnosis of skin diseases by dermatologists.

References

[1] D. Seth, K. Cheldize, D. Brown, and E. F. Freeman, "Global burden of skin disease: Inequities and innovations," Current Dermatology Reports, vol. 6, no. 3, pp. 204–210, 2017.

[2] World Health Organization, "WHO's first global meeting on skin NTDs calls for greater efforts to address their burden," 2023. [Online]. Available: https://www.who.int/news/item/31-03-2023-who-first-global-meeting-on-skin-ntds-calls-for-greater-efforts-to-address-their-burden. [Accessed: Jan. 11, 2025].

[3] World Health Organization, "Radiation: Ultraviolet (UV) radiation and skin cancer," [Online]. Available: https://www.who.int/news-room/questions-and-answers/item/radiation-ultraviolet-(uv)-radiation-and-skin-cancer. [Accessed: Jan. 11, 2025].

[4] Department of Dermatology and Venereology, Chittagong Medical College and Hospital, Bangladesh et al., "The burden of dermatoses: Evidence from Bangladesh," Global Journal of Dermatology and Venereology, vol. 8, no. 1, pp. 10–16, 2020.

[5] M. R. Kabir, M. A. K. Khan, and A. K. Karmakar, "Dermatological patients at the outdoor of an upazila health complex," TAJ Journal of Teachers Association, vol. 17, no. 2, pp. 93–94, 1970.

[6] T.-C. Pham, A. Doucet, C.-M. Luong, C.-T. Tran, and V.-D. Hoang, "Improving skin-disease classification based on customized loss function combined with balanced mini-batch logic and real-time image augmentation," IEEE Access, vol. 8, pp. 150725–150737, 2020.

[7] S. G. Malik, S. S. Jamil, A. Aziz, S. Ullah, I. Ullah, and M. Abohashrh, "High-precision skin disease diagnosis through deep learning on dermoscopic images," Bioengineering, vol. 11, no. 9, p. 867, 2024.

[8] X. Zhang, S. Wang, J. Liu, and C. Tao, "Towards improving diagnosis of skin diseases by combining deep neural network and human knowledge," BMC Medical Informatics and Decision Making, vol. 18, no. S2, 2018.

[9] K. Sriwong, S. Bunrit, K. Kerdprasop, and N. Kerdprasop, "Dermatological classification using deep learning of skin image and patient background knowledge," International Journal of Machine Learning and Computing, vol. 9, no. 6, pp. 862–867, 2019.

[10] Kaggle, "Skin Disease Dataset," [Online]. Available: `https://www.kaggle.com/datasets/pacificrm/skindiseasedataset`. [Accessed: Jan. 11, 2025].

[11] M. N. Hossen, V. Panneerselvam, D. Koundal, K. Ahmed, F. M. Bui, and S. M. Ibrahim, "Federated machine learning for detection of skin diseases and enhancement of internet of medical things (IoMT) security," IEEE Journal of Biomedical and Health Informatics, vol. 27, no. 2, pp. 835–841, 2023.

[12] T. M. Fahrudin and I. Z. A. Illah, "SkinMate: Mobile-based application for detecting multi-class skin diseases classification using pre-trained MobileNetV2 on CNN architecture," in Proceedings of the IEEE 9th Information Technology International Seminar (ITIS), 2023, pp. 1–6.

[13] D. M. Asadujjaman and P. C. Shill, "Cardiovascular disease diagnosis prediction system using machine learning," in Smart Innovation, Systems and Technologies, Singapore: Springer Nature Singapore, 2024, pp. 309–319.

[14] M. J. Ferdous, D. M. Asadujjaman, and M. M. Rahman, "An ensemble deep transfer learning approach for classifying COVID-19, pneumonia, and healthy lungs in chest X-ray images with GRAD-CAM visualization," in 2024 27th International Conference on Computer and Information Technology (ICCIT), 2024, pp. 3075–3080.

[15] M. M. Ikbal et al., "Intelligent Recognition of Bangla Handwritten Digits," in 2025 International Conference on Quantum Photonics, Artificial Intelligence, and Networking (QPAIN), 2025, pp. 1–6.

[16] M. Z. Hasan et al., "A CNN approach to automated detection and classification of brain tumors," in 2025 International Conference on Electrical, Computer and Communication Engineering (ECCE), 2025, pp. 1–6.

[17] F. Ahmmed, M. Z. Raihan, K. Nahar, and D. M. Asadujjaman, "Automated detection and classification method of brain tumors using CNNs and deep transfer learning," in 2025 International Conference on Quantum Photonics, Artificial Intelligence, and Networking (QPAIN), 2025, pp. 1–6.

[18] C. Mitra, M. M. Ikbal, F. Parvin, M. M. Rahman, and D. M. Asadujjaman, "Transfer learning based multiclass brain tumor classification using MRI data," in 2025 International Conference on Quantum Photonics, Artificial Intelligence, and Networking (QPAIN), 2025, pp. 1–6.

[19] M. M. Rahman et al., "Recognizing Bangla numerals: A deep learning approach on a novel handwritten dataset," in Lecture Notes in Networks and Systems, Cham: Springer Nature Switzerland, 2026, pp. 100–111.

[20] A. Tamim, M. W. Jahan, M. R. S. Chowdhury, A. Hossain, M. M. Rahman, and A. H. M. R. Imon, "Machine learning-driven market value prediction for European football players," J. Comput. Math. Data Sci., vol. 15, no. 100118, p. 100118, 2025.